Original Article

Comparison of Peri-Implant Bone Stress with Different Implant Crest Module Designed by 3D Finite Element Analysis

Hsin-Mei Hsieh
Department of Stomatology, Veterans General Hospital, Taipei.
School of Dentistry, National Yang-Ming University, Taiwan.

Ming-Lun Hsu
Professor and Dean
School of Dentistry
National Yang-Ming University

Mail: mlhsu@ym.edu.tw
Tel: +886-2-28212943
Fax: +886-2-28264053

DOI: 10.6926/JPI.201812_7(4).0005

Abstract

Purpose: The mechanism of early implant bone loss is not fully understood, and there is ongoing controversy regarding which implant crest module geometry is more favorable for the preservation of crestal cortical bone. The main purpose of this study was to compare the stress placed on crestal cortical bone by three different types of implant crest module designs: divergent, straight, and convergent designs.

Material and methods: Models of divergent, straight, and convergent implant crest modules including an implant body, prostheses, and portion of the posterior left mandible were fabricated. To simulate osseointegration, the models were designed as if "bonding" had occurred between the implant and alveolar bone. A vertical loading of 200 N was applied over five occlusal contacts to simulate the maximum intercuspal position. An oblique loading of 200 N was applied at two occlusal contacts over the buccal cusps at a 30-degree angle with the direction of buccal to lingual. The stress distribution in the peri-implant bone and the displacement of the implant were then analyzed.

Results: The peak von Mises stress was concentrated around the crestal region of the cortical bone and the bottom of the cortical bone, especially in the convergent model. The maximal von Mises stress values of the divergent, straight, and convergent models were 41.4 MPa, 54.3 MPa, and 62.4 MPa, respectively, during vertical loading and 88 MPa, 90.6 MPa, and 112.6 MPa, respectively, during oblique loading.

Conclusion: Under the limitations of this study, the convergent implant crest module model induced more stress concentrated around the cortical bone and implant crest module area, especially in the oblique loading condition. The shape of an implant crest module may thus play an important role in the stress distribution around bone.

Key words: early implant bone loss, implant crest module, stress distribution, finite element analysis

Introduction

To date, the survival rate of dental implants is about 91~100%, and the success rate is about 84~97%. The most commonly used criterion for implant success, which was proposed by Albrektsson et al.[1] and Smith and Zarb[2], is a marginal bone loss of less than

1.5 mm for the first year and 0.2 mm for each subsequent year, However, the mechanism underlying a marginal bone loss of 1.5 mm or more in the first year is not yet fully understood.

According to the definition proposed by Adell et al.[3], early implant bone loss consists of the marginal bone loss resulting from the combined effects of implant placement and implant loading within the first year. Although the mechanism of early implant bone loss is not fully understood, it has been postulated that a number of factors may influence this process[4], including surgical trauma, microgaps, biologic width, occlusal overload, and the design of the implant crest module. Also, some studies have suggested that stress concentrated at the junction of the implant crest module and crestal cortical bone is related to marginal bone loss[4]. Early implant bone loss is related not only to functional but also esthetic complications, and the esthetic outcomes of implant restoration are regarded as increasingly important nowadays. In any case, it seems likely that implant design and the load distribution at the implant-bone interface play an important role in early implant bone loss, and so these factors should be considered in searching for solutions to prevent or decrease the amount of early implant bone loss.

To prevent or decrease the amount of early implant bone loss, implant manufacturers have modified both the macro- and micro-structures of implants. However, there is ongoing controversy regarding which implant crest module geometry is more favorable for the preservation of crestal cortical bone. There are three types of implant crest module geometries now commercially available: divergent, straight, and convergent (Fig. 1). There is still no consensus, however, as to which kind of implant crest module shape is more favorable for limiting crestal bone loss. The main purpose of this study, therefore, was to compare the stress placed on crestal cortical bone by divergent, straight, and convergent implant crest module designs.

Material and methods

The ANSYS Workbench 15 (ANSYS, Pennsylvania, United States) was used to construct the posterior mandible region. Each bone block used was approximately 12 mm in width bucco-lingually, 27 mm in height inferior-superiorly, and 20 mm in length mesial-distally. Each bone block consisted of cancellous bone surrounded by 1.5 mm thick cortical bone[5](Fig. 2). The length of each implant body was 10 mm, including the 1.5 mm of implant crest module. The coronal part of each implant at bone level was different in order to compare divergent, straight, and convergent shape designs of the implant crest module. The width of the divergent model was 5 mm, the width of the straight model was 4 mm, and the width of the convergent model was 3 mm (Fig. 3). Meanwhile, the diameter below the implant crest module was 4 mm for all the models. The implant thread design had a 0.33 x 0.33 mm square shape with a 0.8 mm screw pitch[6]. The height of the implant abutment was 7 mm with a core area of 5 mm in height for the crown-retained portion[7], while the dimension of the core was 4 mm in the coronal area, the diameter of the abutment was 7.7 mm, and the shoulder margin was 0.5 mm. For simplicity, the implant abutment and implant body were set as a one-piece unit. For implant restoration, a D800 dental laboratory scanner (3Shape, Copenhagen, Denmark) was used to scan a lower left first molar typodont tooth. After that, the typodont image data and implant data were input into Meshmixer 3.2 (Autodesk, California, United States) and combined in order to construct the crown portion. The crown was 11.85 mm in length and 10.55 mm in width. The maximum crown thickness was 2.82 mm. In order to transfer the data to the solid body, FreeCAD 0.16 (Free Software Foundation, Massachusetts, United States) was used to convert the data to the form of a STEP file. Finally, we input the crown portion data into ANSYS Workbench 15 and analyzed the stress distribution.

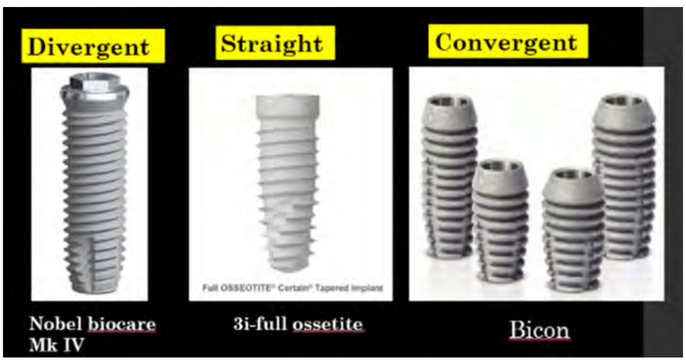

Fig. 1: Three types of implant crest module geometries which are commercially available: divergent, straight and convergent.

Bone is anisotropic in nature[5, 8, 9]. We therefore assumed that the bone was an anisotropic material. The material properties are shown in Table I. The material properties of the crown[10] and implant[11] were assumed to be isotropic, homogeneous, and linearly elastic, and the material properties are shown in Table II. The interface between the bone and implant was set as "bonded" to simulate the stage after socket healing and perfect implant osseointegration. The crown and implant interface were set as bonded without any loosening, while the cement space was neglected[12]. Two types of loading condition were used: axial loading and oblique loading. The axial loading was used to simulate the conditions of the maximum intercuspal position[13,14]. The loading was applied over five occlusal contacts of the lower first molar, including the cusp tip, the crest of the marginal ridge, and the bottoms of the fossae. According to a study by Sultana et al.[15], the average occlusal contact area of the lower first molar is 2.5 mm^2. To simplify the occlusal contact, we assumed the contact areas to be round in shape, with the radius of each being about 0.4 mm. We then used this information to create five occlusal contacts with Meshmixer 3.2 (Fig. 4). For the oblique loading condition, two of the five occlusal contacts of the maximum intercuspal position at the buccal cusp were used to simulate the grinding phase when chewing (Fig. 4). The angulation of the loading force was 30 degrees between the force and the long axis of the tooth, with the direction being buccal to lingual[13, 16].The force applied in both loading conditions was 200 N in order to simulate normal chewing force[17]. For the vertical loading, the force applied to each of the five occlusal contacts was set at 40 N. For the oblique loading, two of the occlusal contacts were chosen, and the force applied to each occlusal contact was set at 100 N and applied at a 30-degree angle with the direction of buccal to lingual. The 200 N of force used in the ANSYS Workbench 15 was "remote force", which is used as an alternative way to apply force to the body. The workbench calculates the equivalent moment and force and applies them to the body. The mesial and distal end of the mandible were set to "fixed support", so that the displacement of nodes in these directions was equal to zero[18].

Results

The number of elements and nodes are shown in Table III.

During vertical loading, the peak von Mises stress was concentrated around the crestal region of the cortical bone and the bottom of the cortical bone, especially in the convergent model. In terms of the occlusal view, the von Mises stress was concentrated on the buccal and lingual area. The maximal von Mises stress values of the divergent, straight, and convergent models were 41.4 MPa, 54.3 MPa, and 62.4 MPa, respectively (Fig. 5).

During oblique loading, the peak von Mises stress was mostly concentrated on the crestal region of the cortical bone and only partially concentrated on the bottom of the cortical bone. In terms of the occlusal view, the von Mises stress was concentrated only on the lingual area. The maximal

Table I

Material properties of cortical and cancellous bone

Material	Young's modulus (MPa)	Poisson's ratio (ν)	Shear modulus (MPa)	Reference
Cortical bone	Ex=17900	ν_{xy}=0.18	G_{xy}=4500	5, 8, 20
	Ey=12500	ν_{yz}=0.31	G_{yz}=5300	
	Ez=26600	ν_{xz}=0.28	G_{xz}=7100	
Cancellous bone	Ex=1148	ν_{xy}=0.055	G_{xy}=68	
	Ey=210	ν_{yz}=0.055	G_{yz}=68	
	Ez=1148	ν_{xz}=0.322	G_{xz}=434	

The x-direction is mesial-lateral, the y-direction is inferio-superior, and the z-direction is anterioe-posterior von Mises stress values of the divergent, straight, and convergent models were 88 MPa, 90.6 MPa, and 112.6 MPa, respectively (Fig. 6).

During vertical loading, the peak von Mises stress of the implant was concentrated on the first thread. The maximal von Mises stress values of the divergent, straight, and convergent implants were 47.5 MPa, 69.1 MPa, and 66.3 MPa, respectively (Fig. 7).

During oblique loading, the peak von Mises stress of the divergent implant was concentrated on the junction between the implant crest module and the implant body. The von Mises stresses of the straight and convergent models were concentrated on the lingual side of the implant crest modules. The maximal von Mises stress values of the divergent, straight, and convergent implants were 94.9 MPa, 127.1 MPa, and 298.2 MPa, respectively (Fig. 8).

During vertical loading, the maximal displacement values of the divergent, straight, and convergent models were 13.7 μm, 15 μm, and 16 μm, respectively, and during oblique loading, the maximal displacement values of the divergent, straight, and convergent models were 31 μm, 37.7 μm, and 51.4 μm, respectively.

Discussion

The results favored the divergent implant crest module, which showed the least stress concentrated on the crestal cortical bone area. Meanwhile, the convergent implant crest module showed the greatest stress concentration.

The first possible reason for these results was the total surface area of each implant crest module. The total surface area of the divergent implant crest module was greater than those of the straight and convergent designs, and when the total surface area is wider, the stress will be distributed more evenly.

The second possible reason for the results was the rigidity of the implant body. Wide diameter implants show less displacement. During vertical loading, the maximal displacement values of the divergent, straight, and convergent models were 13.7 μm, 15 μm, and 16 μm, respectively. The convergent model showed the greatest displacement, which indicates that lower rigidity may have contributed to this result, which would, in turn, eventually cause more stress to be induced at the bone-implant interface. This differences in

Table II

Material properties of implant and crown

Material	Young's modulus (MPa)	Poisson's ratio (ν)	Reference
Implant/abutment (CP Ti grade 4)	102000	0.3	11
Crown (gold alloy)	90000	0.3	10

Table III

Material properties of implant and crown

	Elements	Nodes
Divergent model	100750	170670
Straight model	99925	169251
Convergent model	100645	170543

displacement were even more obvious under the oblique loading condition. During oblique loading, the maximal displacement values of the divergent, straight, and convergent models were 31 μm, 37.7 μm, and 51.4 μm, respetively.

The third possible reason for the results was the geometry of the cortical bone. When the implant crest module is divergent, there is a blunt angle at the top of the cortical bone; when the implant crest module is straight, there is a right angle at the top of the cortical bone; and when the implant crest module is convergent, there is an acute angle at the top of the cortical bone. An acute angle at the top of the cortical bone would induce greater stress concentration than a blunt angle.

Bone is anisotropic in nature[5, 8, 9], which means that its mechanical properties are different when measured in different directions in the same sample. However, a lot of studies have assumed bone to be an isotropic material in their finite element models[19], when in fact, the stress and strain levels in anisotropic bone are higher than those in isotropic bone[20]. In our study, we tried to use models that were close to the reality, so we assumed that bone is an anisotropic material. In order to compare the different implant crest module designs, gold alloy restoration was selected due to its ductile property, which meant that the stress could be more evenly distributed when loading was applied. Because we focused on the stress and strain over the cortical bone area, the cement space could be neglected[12].

The maximal biting force varies from individual to individual, ranging from 8 N ~ 880 N[21]. The average chewing force of an implant restoration is about 200 N at the first molar area [53, 72]. According to a literature review, it appears that most finite element analyses have assumed that occlusal loads are directly applied on the abutment of dental implants[22]. Such studies failed to consider the effect of a prosthetic crown in the clinical setting. The application of a load on a crown or implant leads to different bending moments[23]. Therefore, in our study, we scanned the morphology of a lower left first molar typodont tooth as our implant prosthesis model. Compared to other studies[24], therefore, the morphology of the prostheses used in this study was more close to that of clinical situations. According to Eskitascioglu et al.[25], the location of loading influences the stress distribution. We simulated the maximal intercuspal position as the vertical loading. It is the reason why, when cusp tips contact flat surfaces, the resultant force is directed vertically through the long axis of the teeth[13]. According to optimal occlusion[13, 14], we set up five occlusal contacts in our models. Under oblique loading, the tooth contact during mastication can be divided into the crushing phase and the grinding phase. In the crushing phase, the buccal cusps of the mandibular teeth are almost directly under the buccal cusps of the maxillary teeth. After that, the mandible's movement continues to close the bolus of food between the teeth, which begins the grinding phase. During the grinding phase, the mandible is guided by the occlusal surface of the teeth and moves back to the maximum intercuspal position, which causes the cuspal inclines of the teeth to pass across each other, permitting shearing and grinding of the bolus of food[13]. Therefore, the angulation of the force depends on the inner inclination of the maxillary cusp[16]. The angulation between the force direction and the long axis of the tooth was set to be 30 degrees in this study. Under the oblique loading condition, two occlusal contacts on the buccal cusp of the lower first molar were selected, and the direction of the reaction force was from buccal to lingual[13].

The limitations of this study were as follows: (1) the diameter of the abutment was not constant due to the different implant crest module designs; (2) the same total area with different contours might need to be tested; and (3) the finite element analysis could be applied for mechanical properties, but the relevant biological properties should be confirmed clinically.

Conclusion

Under the limitations of this study, the convergent implant crest module model induced more stress concentrated around the cortical bone and implant crest module area, especially in the oblique loading condition. The shape of an implant crest module may thus play an important role in the stress distribution around the bone.

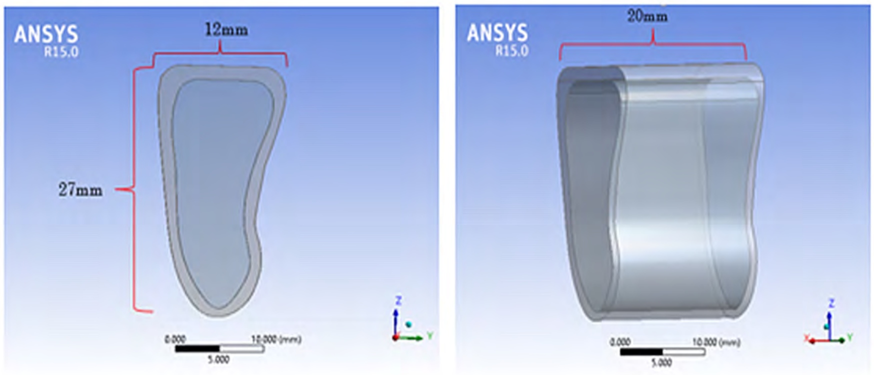

Fig. 2: Bone block : the bone block is approximately 12mm in width bucco-lingually, 27mm in height inferio-superiorly, and 20mm in length mesial-distally. The bone block is consisted of cancellous bone surrounded by 1.5mm thickness of cortical bone.

Fig. 3: The implant body with different implant crest module geometries, from top to down: divergent, straight, and convergent; the diameters of implant platform, from top to down, 5mm, 4mm, 3mm.

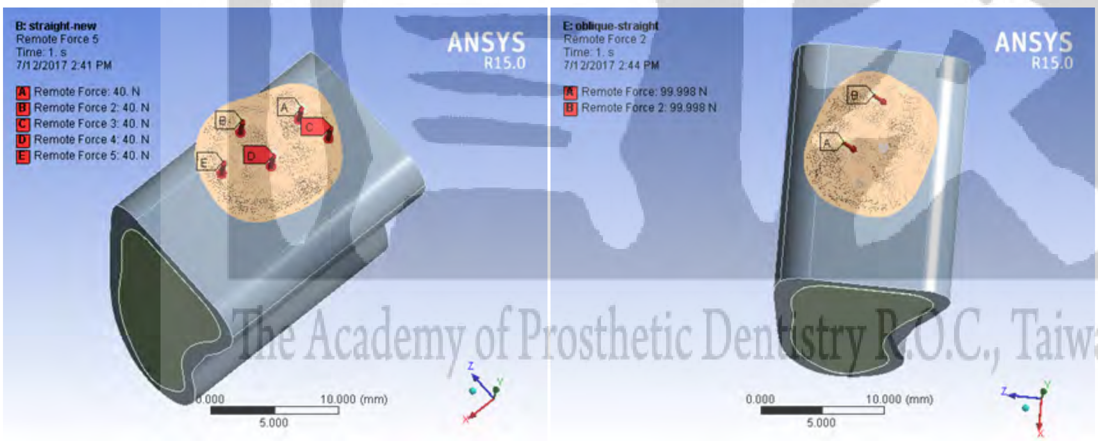

Fig. 4: (left) Under vertical loading, each of the five occlusal contacts was set to be 40 N (right) Each occlusal contact was set to be 100N at 30 degrees with the long axis of the tooth from buccal to lingual.

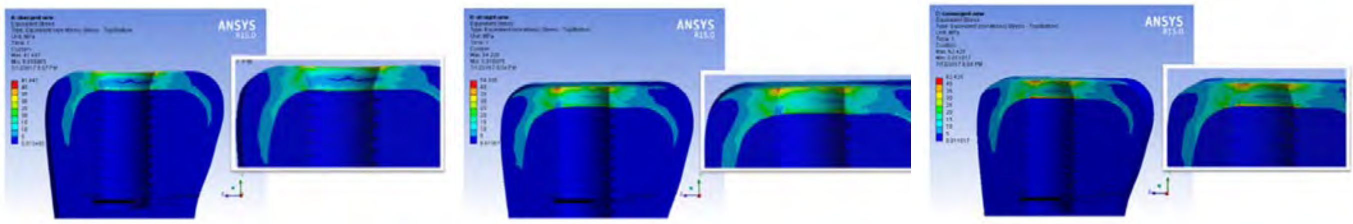

Fig. 5: Under vertical loading condition: distribution of von Mises stress around bone(MPa).

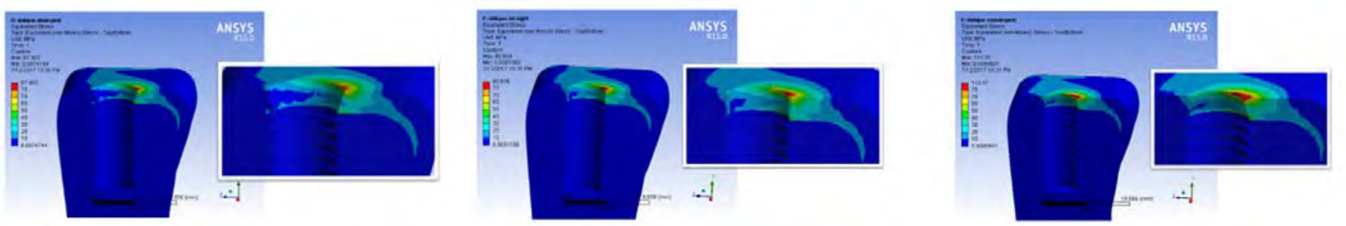

Fig. 6: Under oblique loading condition: distribution of von Mises stress around bone(MPa).

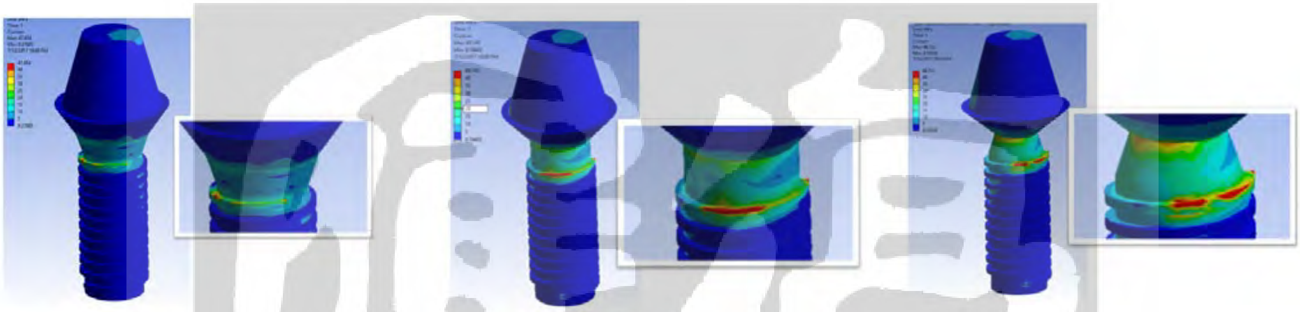

Fig. 7: Under vertical loading condition: distribution of von Mises stress of implant.

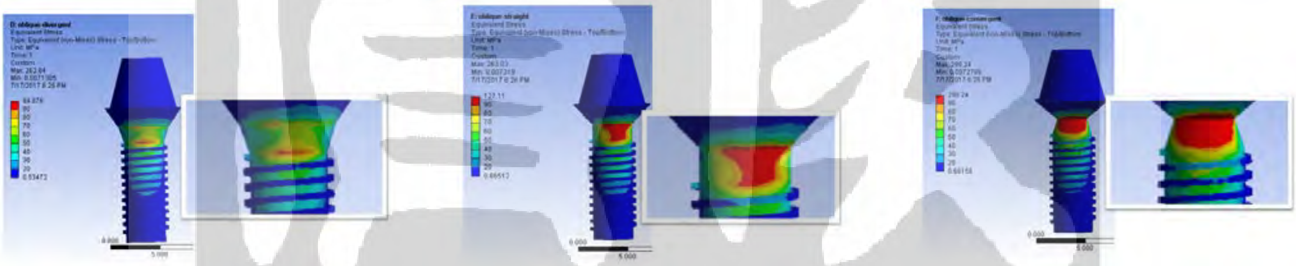

Fig. 8: Under oblique loading condition: distribution of von Mises stress.

References

1. Albrektsson, T., et al., The long-term efficacy of currently used dental implants: a review and proposed criteria of success. Int J Oral Maxillofac Implants, 1986. 1(1): p. 11-25.
2. Smith, D.E. and G.A. Zarb, Criteria for success of osseointegrated endosseous implants. J Prosthet Dent, 1989. 62(5): p. 567-72.
3. Adell, R., et al., A 15-year study of osseointegrated implants in the treatment of the edentulous jaw. Int J Oral Surg, 1981. 10(6): p. 387-416.
4. Oh, T.J., et al., The causes of early implant bone loss: myth or science? J Periodontol, 2002. 73(3): p. 322-33.
5. Schwartz-Dabney, C.L. and P.C. Dechow, Edentulation alters material properties of cortical bone in the human mandible. J Dent Res, 2002. 81(9): p. 613-7.
6. Chang, P.K., et al., Distribution of micromotion in implants and alveolar bone with different thread profiles in immediate loading: a finite element study. Int J Oral Maxillofac Implants, 2012. 27(6): p. e96-101.
7. Misch, C.E., Dental Implant Prosthetics. 2nd ed. 2014: Elsevier Health Sciences.
8. Dechow, P.C., Q. Wang, and J. Peterson, Edentulation alters material properties of cortical bone in the human craniofacial skeleton: functional implications for craniofacial structure in primate evolution. Anat Rec (Hoboken), 2010. 293(4): p. 618-29.
9. O'Mahony, A.M., et al., Anisotropic elastic properties of cancellous bone from a human edentulous mandible. Clin Oral Implants Res, 2000. 11(5): p. 415-21.
10. Benzing, U.R., H. Gall, and H. Weber, Biomechanical aspects of two different implant-prosthetic concepts for edentulous maxillae. Int J Oral Maxillofac Implants, 1995. 10(2): p. 188-98.
11. Tada, S., et al., Influence of implant design and bone quality on stress/strain distribution in bone around implants: a 3-dimensional finite element analysis. Int J Oral Maxillofac Implants, 2003. 18(3): p. 357-68.
12. Proos, K.A., et al., Influence of cement on a restored crown of a first premolar using finite element analysis. Int J Prosthodont, 2003. 16(1): p. 82-90.
13. Okeson, J.P., Management of Temporomandibular Disorders and Occlusion. 2014: Elsevier Health Sciences.
14. Nelson, S.J., Wheeler's Dental Anatomy, Physiology and Occlusion. 2014: Elsevier Health Sciences.
15. Sultana, M.H., K. Yamada, and K. Hanada, Changes in occlusal force and occlusal contact area after active orthodontic treatment: a pilot study using pressure-sensitive sheets. J Oral Rehabil, 2002. 29(5): p. 484-91.
16. Preis, V., et al., Influence of cusp inclination and curvature on the in vitro failure and fracture resistance of veneered zirconia crowns. Clin Oral Investig, 2014. 18(3): p. 891-900.
17. Ferrario, V.F., et al., Single tooth bite forces in healthy young adults. J Oral Rehabil, 2004. 31(1): p. 18-22.
18. Himmlova, L., et al., Influence of implant length and diameter on stress distribution: a finite element analysis. J Prosthet Dent, 2004. 91(1): p. 20-5.
19. Ramos Verri, F., et al., Biomechanical influence of crown-to-implant ratio on stress distribution over internal hexagon short implant: 3-D finite element analysis with statistical test. J Biomech, 2015. 48(1): p. 138-45.
20. O'Mahony, A.M., J.L. Williams, and P. Spencer, Anisotropic elasticity of cortical and cancellous bone in the posterior mandible increases peri-implant stress and strain under oblique loading. Clin Oral Implants Res, 2001. 12(6): p. 648-57.
21. Bates, J.F., G.D. Stafford, and A. Harrison, Masticatory function - a review of the literature. III. Masticatory performance and efficiency. J Oral Rehabil, 1976. 3(1): p. 57-67.
22. Yamanishi, Y., et al., Influences of implant neck design and implant–abutment joint type on peri-implant bone stress and abutment micromovement: Three-dimensional finite element analysis. Dental materials, 2012. 28(11): p. 1126-1133.
23. Falcon-Antenucci, R.M., et al., Influence of cusp inclination on stress distribution in implant-supported prostheses. A three-dimensional finite element analysis. J Prosthodont, 2010. 19(5): p. 381-6.
24. Chang, C.L., C.S. Chen, and M.L. Hsu, Biomechanical effect of platform switching in implant dentistry: a three-dimensional finite element analysis. Int J Oral Maxillofac Implants, 2010. 25(2): p. 295-304.
25. Eskitascioglu, G., et al., The influence of occlusal loading location on stresses transferred to implant-supported prostheses and supporting bone: A three-